

retrieving.html (or from the Cambridge Crystallographic Data Centre, 12, Union Road, Cambridge CB21EZ, UK; fax: (+44) 1223-336-033; or deposit@ccdc.cam.ac.uk).

- [11] For crystal structures of a) [1.1]disila-, b) [1.1]distanna-, c) [1.1]diplumba-, and d) [1.1]digallaferrocenophanes, see a) D. L. Zechel, D. A. Foucher, J. K. Pudelski, G. P. A. Yap, A. L. Rheingold, I. Manners, *J. Chem. Soc. Dalton Trans.* **1995**, 1893–1899; b) A. Clearfield, C. J. Simmons, H. P. Withers, Jr., D. Seyferth, *Inorg. Chim. Acta* **1983**, 75, 139–144; c) G. Utri, K. E. Schwarzahans, G. M. Allmaier, *Z. Naturforsch. B* **1990**, 45, 755–762; d) W. Uhl, I. Hahn, A. Jantschak, T. Spies, *J. Organomet. Chem.* **2001**, 637–639, 300–303; P. Jutzi, N. Lenze, B. Neumann, H.-G. Stammer, *Angew. Chem.* **2001**, 113, 1470–1473; *Angew. Chem. Int. Ed.* **2001**, 40, 1424–1427.
- [12] P. Burk, I. A. Koppel, I. Koppel, R. Kurg, J.-F. Gal, P.-C. Maria, M. Herreros, R. Notario, J.-L. M. Abboud, F. Anvia, R. W. Taft, *J. Phys. Chem. A* **2000**, 104, 2824–2833.
- [13] M. Fontani, F. Peters, W. Scherer, W. Wachter, M. Wagner, P. Zanello, *Eur. J. Inorg. Chem.* **1998**, 1453–1465; M. Fontani, F. Peters, W. Scherer, W. Wachter, M. Wagner, P. Zanello, *Eur. J. Inorg. Chem.* **1998**, 2087.
- [14] a) The cell for voltammetric studies was designed as detailed in ref. [14b]. Voltammetric scans were referenced by addition of a small amount of ferrocene as internal standard at an appropriate time of the experiment. For referencing of the oxidized solution a small sample (ca. 3 mL) was transferred from the electrolysis cell to the voltammetric cell, the required amount of ferrocene added, and voltammetric traces were recorded. Higher electric currents could not be obtained in the CVs due to solubility and adsorption problems; b) R. F. Winter, F. M. Hornung, *Organometallics* **1999**, 18, 4005–4014.
- [15] For general information on the electrochemistry of ferrocenes, see a) P. Zanello in *Ferrocenes* (Eds.: A. Togni, T. Hayashi), VCH, Weinheim, **1995**; b) D. Astruc, *Electron Transfer and Radical Processes in Transition Metal Chemistry*, Wiley-VCH, Weinheim, **1995**.
- [16] Values at $v = 0.2 \text{ V s}^{-1}$. For the internal ferrocene standard, a peak potential difference ΔE_p of 82 mV was obtained under these conditions.
- [17] P. D. Beer, P. A. Gale, G. Z. Chen, *J. Chem. Soc. Dalton Trans.* **1999**, 1897–1909.

Li-Intercalated Oxometallobanes

Intercalation of Alkali Metal Cations into Layered Organotitanium Oxides**

José Gracia, Avelino Martín, Miguel Mena,*
 María del Carmen Morales-Varela, Josep-M. Poblet,
 and Cristina Santamaría

Dedicated to Professor Pascual Royo
 on the occasion of his 65th birthday

Species with a metallobane structure constitute an interesting building block in inorganic solids, and considerable effort has been invested in selecting the composition and geometry of the precursor complexes to obtain specific characteristics and properties.^[1] Some examples of the wide variety of inorganic materials whose structures are based on molecular cubane-like motifs are the molybdenum^[2] and aluminum phosphates,^[3] $M_x Mo_x P_y O_z$ ($M = \text{metal cation}$), or various hydroxometalates $[M_x O_y (\text{OH})_z]L$ ($M = \text{Ge, Ln, ...}$).^[4]

We have reported the formation and structure of the oxoheterometallobanes $[\{(\text{CO})_3\text{Mo}\}(\mu_3\text{-O})_3\{\text{Ti}_3(\eta^5\text{-C}_5\text{Me}_5)_3(\mu_3\text{-CR})\}]$ ($R = \text{H, Me}$)^[5], which were obtained from the preorganized organometallic oxides $[\{\text{Ti}(\eta^5\text{-C}_5\text{Me}_5)(\mu\text{-O})\}_3(\mu_3\text{-CR})]$ ($R = \text{H}$ (**1**), Me (**2**)).^[6] Once we observed that the latter might be involved directly as macrocyclic tridentate ligands in encapsulation processes of different metals, we became interested in incorporating diverse metal complex fragments at the free vertex of the μ_3 -alkylidyne oxo derivatives to build up the corresponding oxoheterometallobanes.

As part of these ongoing studies, here we present the intercalation of alkali metal ions into layered organometallic titanium oxides by treatment of the alkylidyne complex **1** with different alkali metal alkyl and amide reagents.

The one-pot reaction of the tripodal starting material **1** with MR ($M = \text{Li, R} = \text{CH}_2\text{SiMe}_3, \text{CH}_2\text{CMe}_3, n\text{Bu}$; $M = \text{Na, R} = n\text{Bu}$; $M = \text{K, R} = n\text{Bu, CH}_2\text{Ph}$) in toluene/hexane at room temperature leads to the oxoheterometallobanes **3–5** in good yields. These compounds can be also obtained by

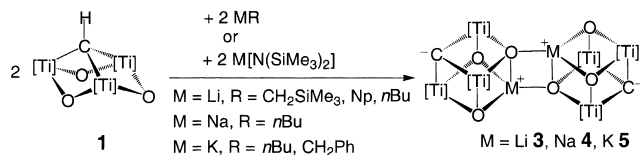
[*] Dr. M. Mena, Dr. A. Martín, M. d. C. Morales-Varela,
 Dr. C. Santamaría
 Departamento de Química Inorgánica
 Universidad de Alcalá, Campus Universitario
 28871 Alcalá de Henares-Madrid (Spain)
 Fax: (+34) 91-885-4683
 E-mail: miguel.mena@uah.es

J. Gracia, Prof. Dr. J.-M. Poblet
 Departament de Química Física i Inorgánica
 Universitat Rovira i Virgili
 Imperial Tarraco 1, 43005 Tarragona (Spain)

[**] Financial support for this work was provided by the Ministerio de Ciencia y Tecnología (BQU2001-1499 and PB98-0916-CO2-02), Universidad de Alcalá (2002/010), and Generalitat de Catalunya (SGR01-00315). M.C.M.-V. thanks the Comunidad de Madrid for a doctoral fellowship.

using $M[N(\text{SiMe}_3)_2]$ ($M = \text{Li}, \text{Na}, \text{K}$) in toluene or hexane at 60°C (Scheme 1).

Crystallization of **3** from a double layer toluene/hexane at room temperature gave dark green crystals suitable for an X-ray diffraction study.^[7–9] A simplified view of the unit cell of **3** showing the intercalation of the lithium atoms into the



Scheme 1. Synthesis of the oxoheterometallic cubanes **3–5**. [Ti] = $\text{Ti}(\eta^5\text{-C}_5\text{Me}_5)$.

organometallic titanium oxide layers is given in Figure 1, and the molecular structure of **3** is shown in Figure 2. The structure reveals two $\text{LiO}_3\text{Ti}_3\text{C}$ cubane cores directly linked through two Li–O bonds. The ensuing Li_2O_2 rhomb is planar and has the dimensions $\text{Li}\cdots\text{Li}$ 2.61(2) Å, (close to the value of 2.67 Å, reported for the diatomic species $\text{Li}_2^{[10]}$), Li–O 2.386(13) and 1.891(12) Å, and O–Li–O 105.7(5)°, consistent with a trigonal-pyramidal LiO_4 coordination of its lithium atoms, analogous to that found for $[\text{M}(\mu_3\text{-N})(\mu_3\text{-NH})_2\{\text{Ti}_3(\eta^5\text{-C}_5\text{Me}_5)_3(\mu_3\text{-N})\}]_2$ ($M = \text{Li}, \text{Na}$).^[11]

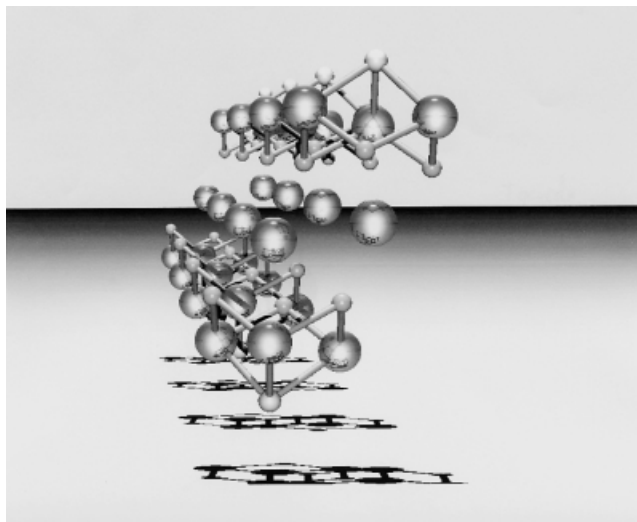


Figure 1. Simplified view of the unit cell of **3**, normal to the (100) plane.

The $\text{Ti}_3\text{O}_3\text{C}$ subunits of **3** display several structural differences to that of the parent compounds **1** and **2**. The angles Ti–O–Ti (av 95.4°) and O–Ti–O (av 96.4°) in **3** are smaller than those in **1** and **2** (Ti–O–Ti av 100°, O–Ti–O av 104°).^[6a,c] The Ti–C1 bond length (av 2.055 Å) lies between those in **1** (Ti–C1 2.10 Å)^[6c] and **2** (Ti–C1 2.12 Å).^[6a,c] and that in the zwitterionic derivative $[\{\text{Ti}(\eta^5\text{-C}_5\text{Me}_5)(\mu\text{-O})\}_3\{\mu_3\text{-}\eta^2\text{-C-C}(\text{Me})\text{N}^+(2,6\text{-Me}_2\text{C}_6\text{H}_3)\}]$ (Ti–C 2.017(5) Å).^[12]

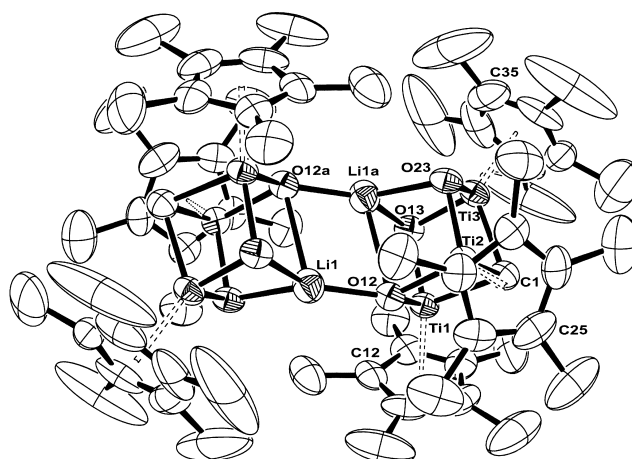


Figure 2. Structure of **3** (ORTEP drawing; 50% probability ellipsoids). The complex resides on an inversion center. Selected distances [Å] and angles [°]: Intercubane: Li–Li 2.61(2), Li–O 1.891(12); Li–(μ_4 -O)–Li 74.3(5), (μ_4 -O)–Li–(μ_4 -O) 105.7(5), Ti–O(12)–Li(1) 130.2(4); intracubane: Ti–Ti 2.798(1) av, Li–Ti 2.885(11) av, (μ_4 -O)–Li 2.386(13) av, (μ_3 -O)–Li 2.057(12) av, Ti–O 1.891(4) av, Ti–C1 2.055(6) av; Ti–C1–Ti 85.8(2) av, C1–Ti–O 89.1(2) av, Ti–O–Ti 95.4(2) av, O–Ti–O 96.4(2) av, Ti–O12–Li1a 87.6(3) av, Ti3–O13–Li1a 86.1(4), Ti1–O13–Li1a 98.1(4), Ti3–O23–Li1a 87.5(4), Ti2–O23–Li1a 98.1(4).

DFT calculations reproduced quite well the X-ray geometry found for **3**.^[13–17] However, for the central rhombic unit the optimization process yielded a structure with two short and two long Li–O bonds of 1.901 and 2.169 Å, respectively. Whereas the short bonds compare well with the experimental distance (1.891 Å), the discrepancy for the long bonds seems excessive (0.22 Å). In spite of this, we found that the energy difference between the complex optimized by keeping the central parallelepiped fixed at the experimental geometry and the fully optimized complex is only 12 kJ mol^{–1}.

The solid compounds **3–5** proved stable under argon at room temperature and practically insoluble in most common solvents (e.g. toluene, hexane, dichloromethane) with the exception of THF, which allowed the characterization of **4** and **5** by NMR spectroscopy. ¹H NMR spectra in $[\text{D}_8]\text{THF}$ of **4** and **5** show only one signal at $\delta = 1.95$ and 1.94 ppm, respectively, which is assigned to the $\eta^5\text{-C}_5\text{Me}_5$ groups. The ¹³C NMR spectra display signals with the appropriate multiplicity for the $\eta^5\text{-C}_5\text{Me}_5$ ligands, as well as a singlet for the apical μ_3 -carbon atom ($\delta = 586.7$ (**4**) and 582.0 ppm (**5**)). These data indicate the removal of the proton of the μ_3 -methylidyne fragment and are consistent with the formulation of these diamagnetic compounds as $[\{\text{M}(\mu_3\text{-O})_3\{\text{Ti}_3(\eta^5\text{-C}_5\text{Me}_5)_3(\mu_3\text{-C})\}]_2$ ($M = \text{Li}, \text{Na}, \text{K}$). Previously, Cummins et al. reported the formation of the carbidomolybdenum(vi) anions $[\{(\text{Ar})\text{RN}\}_3\text{Mo}\equiv\text{C}]^-$ ($R = \text{C}(\text{CD}_3)_2\text{CH}_3$ or *t*Bu; $\text{Ar} = 3,5\text{-Me}_2\text{C}_6\text{H}_3$), which displayed a carbide chemical shift in the range $\delta = 474\text{–}501$ ppm.^[18]

To clarify the magnitude of the chemical shifts found for the apical carbon atom in compounds **4** and **5**, we performed DFT-GIAO-based NMR calculations.^[19] The computed δ value for the apical methylidyne-carbon atom in the precursor tridentate ligand model $[\{\text{Ti}(\eta^5\text{-C}_5\text{H}_5)(\mu\text{-O})\}_3(\mu_3\text{-CH})]$ (**1**) was

Table 1: Experimental and calculated ^{13}C chemical shifts (δ) for the apical carbon atom.

Molecule	δ	$\delta(\text{DFT-GIAO})^{[b]}$	Shielding $^{[a]}$	
			$\sigma_d^{[c]}$	$\sigma_p^{[d]}$
$\{[\text{TiCp}^*(\mu\text{-O})]_3(\mu_3\text{-CH})\}$ (1)	383.2			
$\{[\text{TiCp}(\mu\text{-O})]_3(\mu_3\text{-CH})\}$ (1')		385.3	241.2	-444.2
$\{[\text{MeLi}](\mu_3\text{-O})_3[\text{Ti}_3\text{Cp}_3(\mu_3\text{-CH})]\}$		400.6	243.0	-461.3
$[\text{Li}(\mu_3\text{-O})_3\{\text{Ti}_3\text{Cp}_3(\mu_3\text{-C})\}]$		572.2	254.2	-644.1
$\{[\text{Li}(\mu_3\text{-O})_3[\text{Ti}_3\text{Cp}_3(\mu_3\text{-C})]\}_2$ (3')		572.5	256.4	-646.6
$\{[\text{Na}(\mu_3\text{-O})_3[\text{Ti}_3\text{Cp}_3^*(\mu_3\text{-C})]\}_2$ (4)	586.7			
$\{[\text{K}(\mu_3\text{-O})_3[\text{Ti}_3\text{Cp}_3^*(\mu_3\text{-C})]\}_2$ (5)	582.0			

[a] Shielding in ppm relative to TMS. [b] $\delta = \sigma(\text{TMS}) - (\sigma_d + \sigma_p)$ where the computed $\sigma(\text{TMS})$ is 182.3 ppm. For a detailed description of the implementation of the GIAO method in the ADF package as well as the calculation procedure of σ_d and σ_p see reference [19]. [c] Diamagnetic shielding. [d] Paramagnetic shielding.

385.3 ppm, a value that is almost identical to the experimental value found for **1** ($\delta = 383.2$ ppm). The formation of the carbido species induces an increase of the calculated δ value to 572.2 ppm, which is consistent with the experimental values measured for **4** ($\delta = 586.7$ ppm) and **5** ($\delta = 582.0$ ppm). These latter values can be explained in terms of a predominant paramagnetic contribution (Table 1), which could be attributed to the larger magnetic coupling between the σ carbon lone pair and the titanium orbitals. In the $[\{\text{Ti}(\eta^5\text{-C}_5\text{H}_5)(\mu\text{-O})\}_3(\mu_3\text{-C})]^-$ ionic fragment the HOMO orbital (-4.9 eV) is essentially the apical carbon lone pair, whereas in the corresponding nondeprotonated form $[\{\text{Ti}(\eta^5\text{-C}_5\text{H}_5)(\mu\text{-O})\}_3(\mu_3\text{-CH})]$ (**1'**), this orbital localizes very much lower in energy (at ~ -8 eV).

Because non-intermediates were detected during the course of this reaction, we used DFT calculations to propose the possible sequence leading to the formation of the oxometallobicubane model $[\text{Li}(\mu_3\text{-O})_3\{\text{Ti}_3(\eta^5\text{-C}_5\text{H}_5)_3(\mu_3\text{-C})\}]_2$ (**3'**; Figure 3). The initial step proceeds by coordination of the LiR unit to the oxomethylidyne ligand **1'** (Figure 3). The next step would consist in the CH_4 (or NH_3) elimination by deprotonation at the μ_3 -methylidyne carbon atom, affording

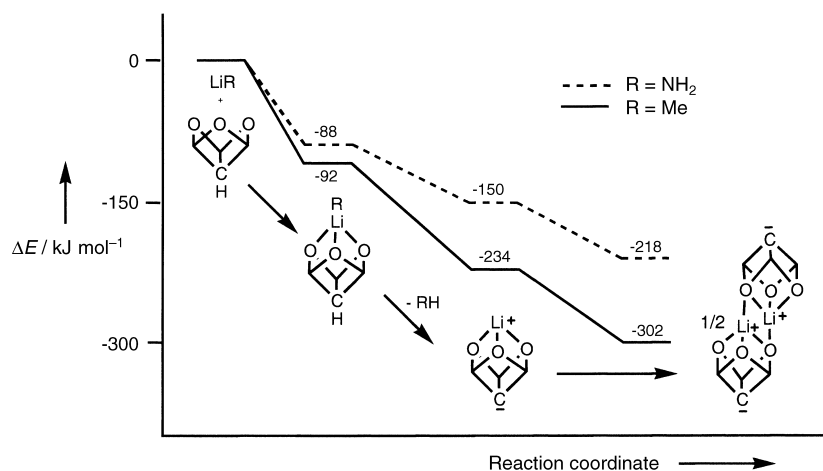


Figure 3. Computed ΔE (kJ mol^{-1}) values for the formation steps of the oxoheterometallobicubane model $\{[\text{Li}(\mu_3\text{-O})_3[\text{Ti}_3(\eta^5\text{-C}_5\text{H}_5)_3(\mu_3\text{-C})]\}_2$ (**3'**).

the monomer complex $[\text{Li}(\mu_3\text{-O})_3\{\text{Ti}_3(\eta^5\text{-C}_5\text{H}_5)_3(\mu_3\text{-C})\}]$. Finally, the assembly of two monomers leads to **3'**. All the processes are exothermic, especially those for the methane elimination.

The slow formation of the μ_3 -ethylidyne complex $[\text{Ti}_3(\eta^5\text{-C}_5\text{Me}_5)_3(\mu_3\text{-O})_3(\mu_3\text{-CMe})]$ (**2**) from the reactions of **3–5** in $[\text{D}_6]$ benzene with MeI confirmed unequivocally the existence of the μ_3 -carbido group.

Herein we have focused on the reactions of the μ_3 -methylidyne species **1** with alkali metal (Li, Na, K) alkyl or amide reagents. The process was analyzed by DFT calculations and the magnitude of the chemical shifts was determined for the apical μ_3 -carbido groups in the products $\{[\text{M}(\mu_3\text{-O})_3[\text{Ti}_3(\eta^5\text{-C}_5\text{Me}_5)_3(\mu_3\text{-C})]\}_2$ ($\text{M} = \text{Li, Na, K}$). As an extension of this work and to gain knowledge on the structural and electronic properties of this kind of compounds, we are currently investigating oxometallobicubane-type systems containing the heaviest alkali metals as well as the incorporation of alkaline-earth metals into these systems.

Experimental Section

3: Treatment of **1** with $\text{Li}[\text{N}(\text{SiMe}_3)_2]$, NpLi , $\text{Li}[\text{CH}_2\text{SiMe}_3]$, or BuLi led to the formation of compound **3**. The reaction of **1** with BuLi is reported as an example. A solution of **1** (0.32 g, 0.52 mmol) in toluene (15 mL) and BuLi (0.3 mL, 0.52 mmol) in hexane (30 mL) was placed in a 100-mL Carious tube with a Young valve. The reaction mixture was left at room temperature overnight, after which a green microcrystalline solid was observed at the bottom of the flask. The solid was filtered and washed with hexane to yield **3** (0.30 g, 94%). This complex decomposed in THF precluding its characterization by NMR spectroscopy; IR (KBr): $\tilde{\nu} = 2907$ (vs), 2856 (vs), 1491 (w), 1437 (s), 1373 (s), 1023 (m), 801 (w), 681 (vs), 616 (vs), 464 (w), 416 cm^{-1} (s); elemental analysis calcd (%) for $\text{Ti}_6\text{O}_6\text{C}_{62}\text{H}_{90}\text{Li}_2$ (1232.50): C 60.41, H 7.36; found: C 60.40, H 7.34.

4: The treatment of **1** with BuNa or $\text{Na}[\text{N}(\text{SiMe}_3)_2]$ afforded compound **4**. The reaction of **1** with $\text{Na}[\text{N}(\text{SiMe}_3)_2]$ is reported as an example. A 100-mL Carious tube with a Young valve was charged with **1** (0.3 g, 0.49 mmol), $\text{Na}[\text{N}(\text{SiMe}_3)_2]$ (0.09 g, 0.49 mmol), and toluene (40 mL). The reaction mixture was heated at 60°C overnight and the red solid formed was washed with hexane to give **4** (0.18 g, 58%); ^1H NMR (300 MHz, $[\text{D}_8]$ THF, 25°C , TMS): $\delta = 1.95$ ppm (s; C_5Me_5); ^{13}C NMR (300 MHz, $[\text{D}_8]$ THF, 25°C , TMS): $\delta = 11.7$ (C_5Me_5), 115.4 (C_5Me_5), 586.7 ppm ($\mu_3\text{-C}$); IR (KBr): $\tilde{\nu} = 2907$ (vs), 2850 (vs), 1493 (w), 1437 (s), 1372 (s), 1023 (m), 795 (w), 681 (vs), 621 (vs), 467 (w), 411 cm^{-1} (s); elemental analysis calcd (%) for $\text{Ti}_6\text{O}_6\text{C}_{62}\text{H}_{90}\text{Na}_2$ (1264.60): C 58.79, H 7.32; found: C 58.90, H 7.39.

5: Analogously to the preparation of **4**, **1** (0.30 g, 0.49 mmol) and $\text{K}[\text{N}(\text{SiMe}_3)_2]$ (0.10 g, 0.49 mmol) were allowed to react in hexane (40 mL) to afford **5** as a red solid (0.21 g, 66%); ^1H NMR (500 MHz, $[\text{D}_8]$ THF, 25°C , TMS): $\delta =$

1.94 ppm (s, C₅Me₅); ¹³C NMR (500 MHz, [D₈]THF, 25 °C, TMS): δ = 11.5 (C₅Me₅), 115.1 (C₅Me₅), 582.0 ppm (μ₃-C); IR (KBr): ν̄ = 2910 (vs), 2857 (vs), 1597 (w), 1495 (w), 1439 (s), 1375 (s), 1247 (w), 1067 (w), 916 (m), 899 (m), 852 (s), 784 (vs), 680 (s), 624 (m), 573 (m), 411 cm⁻¹ (s); elemental analysis calcd (%) for Ti₆O₆C₆₂H₉₀K₂ (1296.82): C 57.42, H 6.99; found: C 56.99, H 7.10.

Received: July 24, 2002

Revised: October 16, 2002 [Z19810]

- [1] A. P. Alivisatos, P. F. Barbara, A. W. Castleman, J. Chang, D. A. Dixon, M. L. Klein, G. L. McLendon, J. S. Miller, M. A. Ratner, P. J. Rossky, S. I. Stupp, M. E. Thompson, *Adv. Mater.* **1998**, *10*, 1297–1336.
- [2] a) R. C. Haushalter, *J. Chem. Soc. Chem. Commun.* **1987**, 1566–1568; b) K. H. Lii, R. C. Haushalter, C. J. O'Connor, *Angew. Chem.* **1987**, *99*, 574–576; *Angew. Chem. Int. Ed. Engl.* **1987**, *26*, 549–551.
- [3] P. Feng, X. Bu, G. D. Stucky, *Science* **1997**, *278*, 2080–2088.
- [4] a) H. Li, M. Eddaoudi, O. M. Yaghi, *Angew. Chem.* **1999**, *111*, 682–685; *Angew. Chem. Int. Ed.* **1999**, *38*, 653–655; b) B.-Q. Ma, D.-S. Zhang, S. Gao, T.-Z. Jin, C.-H. Yan, G.-X. Xu, *Angew. Chem.* **1999**, *111*, 3790–3792; *Angew. Chem. Int. Ed.* **2000**, *39*, 3644–3646.
- [5] A. Abarca, M. Galakhov, P. Gómez-Sal, A. Martín, M. Mena, J. M. Poblet, C. Santamaría, J. P. Sarasa, *Angew. Chem.* **2000**, *112*, 544–547; *Angew. Chem. Int. Ed.* **2000**, *39*, 534–537.
- [6] a) R. Andrés, M. Galakhov, A. Martín, M. Mena, C. Santamaría, *Organometallics* **1994**, *13*, 2159–2163; b) R. Andrés, M. Galakhov, A. Martín, M. Mena, C. Santamaría, *J. Chem. Soc. Chem. Commun.* **1995**, 551–552; c) R. Andrés, PhD thesis, Universidad de Alcalá, Madrid, **1995**.
- [7] X-ray crystal structure determination of **3**: All data were collected on an ENRAF NONIUS CAD4 diffractometer at room temperature, MoK α = 0.71073 Å. The structure was solved, using the WINGX^[8] package, by direct methods (SHELXS-97) and refined by least-squares against F^2 (SHELXL-97).^[9] X-ray data for C₆₂H₉₀Li₂O₆Ti₆ (**3**): 0.45 × 0.34 × 0.30 mm³, triclinic, $P\bar{1}$, $a = 11.405(2)$, $b = 11.695(2)$, $c = 14.671(3)$ Å, $\alpha = 111.71(2)$, $\beta = 90.78(2)$, $\gamma = 116.39(3)^\circ$, $V = 1590.9(5)$ Å³, $\rho_{\text{calcd}} = 1.287$ Mg m⁻³. Intensity measurements were performed by ω - 2θ scans in the range $3^\circ < \theta < 23^\circ$, of the 4789 measured reflections, 4530 were independent; $R1 = 0.056$ and $wR2 = 0.138$ (for 2617 reflections with $F > 4\sigma(F)$). The values of $R1$ and $wR2$ are defined as follows: $R1 = \sum ||F_o| - |F_c|| / \sum |F_o|$; $wR2 = \{[\sum w(F_o^2 - F_c^2)^2] / [\sum w(F_o^2)]\}^{1/2}$. Largest difference peak and hole 0.380 and -0.318 e Å⁻³. All non-hydrogen atoms were anisotropically refined. The hydrogen atoms were positioned geometrically and refined by using a riding model in the last cycles of refinement with a fixed value of $U(\text{eq}) = 0.08$. CCDC-190221 contains the supplementary crystallographic data for this paper. These data can be obtained free of charge via www.ccdc.cam.ac.uk/conts/retrieving.html (or from the Cambridge Crystallographic Data Centre, 12, Union Road, Cambridge CB21EZ, UK; fax: (+44) 1223-336-033; or deposit@ccdc.cam.ac.uk).
- [8] WinGX: L. J. Farrugia, *J. Appl. Crystallogr.* **1999**, *32*, 837–838.
- [9] G. M. Sheldrick, SHELX-97, *Program for Crystal Structure Analysis* (Release 97-2), University of Göttingen, Göttingen, Germany, **1998**.
- [10] W. L. Jolly, *Modern Inorganic Chemistry*, 2nd ed., McGraw-Hill, New York, **1991**, p. 107.
- [11] M. García-Castro, A. Martín, M. Mena, A. Pérez-Redondo, C. Yélamos, *Chem. Eur. J.* **2001**, *7*, 647–651.
- [12] R. Andrés, M. Galakhov, M. P. Gómez-Sal, A. Martín, M. Mena, C. Santamaría, *Chem. Eur. J.* **1998**, *4*, 1206–1213.
- [13] All DFT calculations were carried out with the ADF program^[14] by using triple- ζ and polarization Slater basis sets to describe the valence electrons of C, O, and Li. For titanium, a frozen core composed of the 1s, 2s, and 2p orbitals was described by double- ζ Slater functions, the 3d and 4s orbitals by triple- ζ functions, and the 4p orbital by a single orbital. The geometries and binding energies were calculated with gradient corrections. We used the local spin density approximation, characterized by the electron gas exchange (X α with $a = 2/3$) together with Vosko–Wilk–Nusair parametrization^[15] for correlation. Becke's nonlocal corrections^[16] to the exchange energy and Perdew's nonlocal corrections^[17] to the correlation energy were added.
- [14] a) ADF 2000.01, Department of Theoretical Chemistry, Vrije Universiteit, Amsterdam; b) E. J. Baerens, D. E. Ellis, P. Ros, *Chem. Phys.* **1973**, *2*, 41–51; c) L. Versluis, T. Ziegler, *J. Chem. Phys.* **1988**, *88*, 322–328; d) G. Te Velde, E. J. Baerens, *J. Comput. Phys.* **1992**, *99*, 84–98; e) C. Fonseca Guerra, J. G. Snijders, G. Te Velde, E. J. Baerens, *Theor. Chem. Acc.* **1998**, *99*, 391–403.
- [15] S. H. Vosko, L. Wilk, M. Nusair, *Can. J. Phys.* **1980**, *58*, 1200–1211.
- [16] a) A. D. Becke, *J. Chem. Phys.* **1986**, *84*, 4524–4529; b) A. D. Becke, *Phys. Rev. A* **1988**, *38*, 3098–3100.
- [17] a) J. P. Perdew, *Phys. Rev. B* **1986**, *33*, 8822–8824; b) J. P. Perdew, *Phys. Rev. B* **1986**, *34*, 7406–7406.
- [18] a) J. C. Peters, A. L. Odom, C. C. Cummins, *Chem. Commun.* **1997**, 1995–1996; b) J. B. Greco, J. C. Peters, T. A. Baker, W. M. Davis, C. C. Cummins, G. Wu, *J. Am. Chem. Soc.* **2001**, *123*, 5003–5013.
- [19] a) G. Schreckenbach, T. Ziegler, *J. Phys. Chem.* **1995**, *99*, 606–611; b) Y. Ruiz-Morales, G. Schreckenbach, T. Ziegler, *J. Phys. Chem.* **1996**, *100*, 3359–3367; c) Y. Ruiz-Morales, G. Schreckenbach, T. Ziegler, *Organometallics* **1996**, *15*, 3920–3923; d) G. Schreckenbach, T. Ziegler, *Int. J. Quantum Chem.* **1997**, *61*, 899–918.